AIMS Materials Science, 5(4): 756–769.
DOI: 10.3934/matersci.2018.4.756
Received: 09 April 2018
Accepted: 20 August 2018
Published: 24 August 2018

http://www.aimspress.com/journal/Materials

Research article

Cooling effects of infrared radiative inorganic fillers in heat dissipation coatings at temperatures below 400 K

Satoshi Nakamura[1], Eiji Iwamura[2], Yasuyuki Ota[1] and Kensuke Nishioka[1,*]

[1] Interdisciplinary Graduate School of Agriculture and Engineering, University of Miyazaki, Miyazaki, Japan
[2] R & D Center, PELNOX, LTD., Hadano, Japan

*** Correspondence:** Email: nishioka@cc.miyazaki-u.ac.jp; Tel: +81985587774.

Abstract: Heat dissipation for electronic devices has attracted extensive interest because the reliability, lifetime, and performance are seriously affected by temperature increases during the operation. The effects of inorganic fillers in heat dissipation coatings on the temperature reduction of heat sources between 310 and 400 K were investigated. Acrylic coating films with calcium fluoride, pyrolytic boron nitride, and silicon carbide particle fillers were formed on pristine aluminum plates that were then heated in a closed system. A significant temperature reduction of about 17 K was obtained at the surface of a heat source with an acrylic coating film including calcium fluoride particles on the aluminum plate; under equivalent conditions, the uncoated aluminum plate temperature reached 373 K. The materials used in the coatings were characterized by wavelength-dependent infrared absorption and emission properties. Although the overall emissivity in wide wavelength range is previously considered to be the most crucial variable in radiative cooling, materials have specific infrared absorption and emission properties depending on their physical structures. Therefore, elucidating the relationship between the characteristics of an individual heat emission material and its cooling effects is necessary in order to design more effective heat dissipation measures based on radiation. It was confirmed that the selection of an appropriate filler material with specific infrared emission properties corresponding to the emitting wavelength at the given temperature of the objects to be cooled was important. Distinctive radiative cooling effects were thus obtained, even in the relatively low-temperature range examined here, by the selection of appropriate materials with radiative properties in the temperature range of interest.

Keywords: heat dissipation; coating; filler; resin; cooling

1. Introduction

Heat dissipation for electronic equipment such as semiconductor devices, light-emitting diodes, batteries, and photovoltaics has attracted extensive interest because the reliability, lifetime, and performance are seriously affected by temperature increases during the operation of such equipment [1–5]. With progressively increasing functionality and miniaturization, as demonstrated by recent microprocessors, the heat generated by such devices has increased with increases in the power consumption per component. Therefore, the dissipation of thermal energy accumulated within electronic equipment has become critical. Various thermal management solutions using not only heat transportation but also thermal storage via phase-change materials, have been proposed [6–9]. Simple methodologies utilizing thermal conduction, convection, and radiation are in particularly high demand for practical, efficient, and economical cooling in the operating temperature ranges <373 K of most electronic devices.

Conventional heat dissipation methods for electronic equipment have focused mainly on thermal conduction and convection. Thermal energy derived from a heat source is transported through a heat spreader to either the top surface of the device or a heat reservoir. Because prompt transfer of the thermal energy to a heat sink or top surface is necessary, the thermal conductivity is the most important parameter for conductive cooling. Al and Cu are the most common materials used as heat spreaders because they have high thermal conductivities, excellent formability, and a low cost [10]. Sheet-form graphite and hexagonal boron nitride (h-BN) with highly anisotropic thermal conductivities were recently employed in heat spreaders [11–14]. Carbon-based materials such as diamond, carbon nanotubes, and graphene are emerging as effective alternatives with extremely high thermal conductivities, low weights, and good durability [15–21].

Thermal energy transported by conduction must be expelled from surfaces to the ambient atmosphere, either naturally or by force. The surface roughness and heat transfer coefficient are critical in determining the efficiency of convective cooling. Increasing the surface area using fins and increasing heat transfer coefficients by forced convection using electrical cooling fans are traditional measures that can be applied to portable electronics [22]. However, with size reduction of mobile products, securing space for the installation of conventional heat spreaders, cooling fins, or electric fans inside these products is becoming difficult. Furthermore, as products become smaller and more densely equipped, completely sealed housings are used more frequently to avoid the problems caused by fine particulate matter. In addition, convective heat dissipation cannot occur easily within such closed and confined spaces.

The third mode of heat transfer, radiation, has not been considered seriously as a cooling mechanism for relatively low temperature ranges below 373 K, because the energy flux by radiative heat transfer is proportional to the fourth power of temperature, in accordance with the Stefan–Boltzmann law. However, radiative cooling does occur in winter in dry air. Significant cooling effects below the ambient temperature have been reported by using selective infrared radiation [23–27]. Recently, effective radiative cooling, even under direct sunlight, was reported using a multilayer coating comprising heat-radiating and heat-reflecting layers [28–30]. When heat dissipation coatings with optimized heat emission properties were used, the temperature of a solar cell in a concentrator photovoltaic (CPV) module was reported to decrease by 10 K, while its conversion efficiency improved by 0.5% (from 21.5 to 22.0%) [31]. Thermal energy is dissipated in the form of electromagnetic waves; therefore, a material medium for thermal energy is not required

for radiative cooling. Thermal energy can be directly transported from a heat source to a heat sink, irrespective of an adjacent ambient environment. Because the temperature can be reduced to a point lower than that of the immediate ambient environment, radiative cooling is considered effective for objects in closed and confined systems.

In this study, a material design for radiative heat dissipating coatings was investigated. The coatings were composed of inorganic particles that absorbed and emitted thermal energy and binder resins that adhered to substrates. Because such polymer-based composite materials can be used irrespective of the shapes of heat-generating articles, they are practical in varied applications. Various combinations of fillers and polymers were investigated by considering the thermal conductivity and heat radiation [32–37]. Although the overall emissivity in the wide wavelength range is previously considered to be the most crucial variable in radiative cooling, materials have specific infrared absorption and emission properties depending on their physical structures. Therefore, elucidating the relationship between the characteristics of an individual heat emission material and its cooling effects is necessary in order to design more effective heat dissipation measures based on radiation. Inorganic fillers of calcium fluoride (CaF_2), pyrolytic boron nitride (p-BN), and silicon carbide (SiC), each having characteristic infrared absorption and emission properties, were examined. Focusing on the temperature range between 310 and 400 K, the cooling effects of the composite heat dissipation coatings on Al substrates were discussed.

2. Materials and method

The binder resin and inorganic infrared-absorbing fillers were introduced to a container and mixed by stirring, accompanied by the crushing of visibly observable aggregates. Subsequently, an organic solvent was added to form slurry with the low viscosity of ~500 mPa s. The slurry was uniformly mixed using a homogenizer.

Table 1 shows the compositions of the test samples. The acrylic resin contains ~5 wt% melamine resin as a hardener. The inorganic fillers were selected based on their infrared emission properties, because the emissivity and absorptivity of any solid surface at a given temperature are equivalent when the radiation is in equilibrium with the solid surface, in accordance with Kirchhoff's law. CaF_2, p-BN, and SiC show strong infrared emission peaks at wavelengths of 9.4 μm, 7.3 μm, and >10 μm, respectively. Fourier-transform infrared spectroscopy (FT-IR: AVATAR 360, UMA150 manufactured by Thermo Fisher Scientific Inc.) was used to characterize the infrared emission properties in the wavelength range between 2.0 and 14.0 μm.

Table 1. Compositions of test samples.

Sample no.	Heat dissipation filler	Binder (acrylic) resin	Xylene solvent
A	nil	48.0 vol%	52.0 vol%
B	CaF_2 (18.9 vol%)	20.5 vol%	60.6 vol%
C	p-BN (27.1 vol%)	28.0 vol%	44.9 vol%
D	SiC (26.5 vol%)	26.5 vol%	47.0 vol%

The slurry was spray-coated onto one side of a substrate of pristine Al (A-1050P) to form a heat dissipation coating film. Each substrate was 50 mm wide, 120 mm long, and 2 mm thick. The coating films were cured in an oven at 437 K for 20 min. Microstructures and surface roughness values of the films were characterized by cross-sectional scanning electron microscopy (SEM) and confocal laser microscopy, respectively. The film thickness after curing was approximately 40 μm.

Figure 1 illustrates the apparatus used to evaluate the heat dissipation effects of the coatings. This system simulates an electronic device that generates heat in a package. A heat source of a shunt-type 1-Ω resistor (PBH1ΩD manufactured by PCN, INC.) was firmly fixed at the center of the back side of the Al substrate by a screw pin and a heat-conducting adhesive. The test elements were mounted on a frame built from a thermally insulating material and placed in a closed box made of glass. Carbon sheets as heat insulators were attached inside the box in order to obviate the influx of radiative heat from outside the measurement system. The carbon sheet absorbs the inflow energy from the outside of the measurement system and plays the role of a heat sink which absorbs energy from the heat source in the system. Furthermore, the carbon sheet emits heat to the outside. In this study, the measurement system was placed in an environment with little external heat inflow. As a result, measurement under the designated condition without being influenced by factors from outside of the system was possible. In order to keep the measurement environment constant, it is necessary to release thermal energy from the measurement system to the outside of the system. If there is a material with low emissivity at the boundary of the system, heat may be reflected into the system and the temperature in the system may increase. The measured carbon sheet temperature (T_{carbon}) was kept constant and almost same as ambient temperature ($T_{ambient}$) in the steady state, and it was possible to conduct the experiment under the constant system temperature condition.

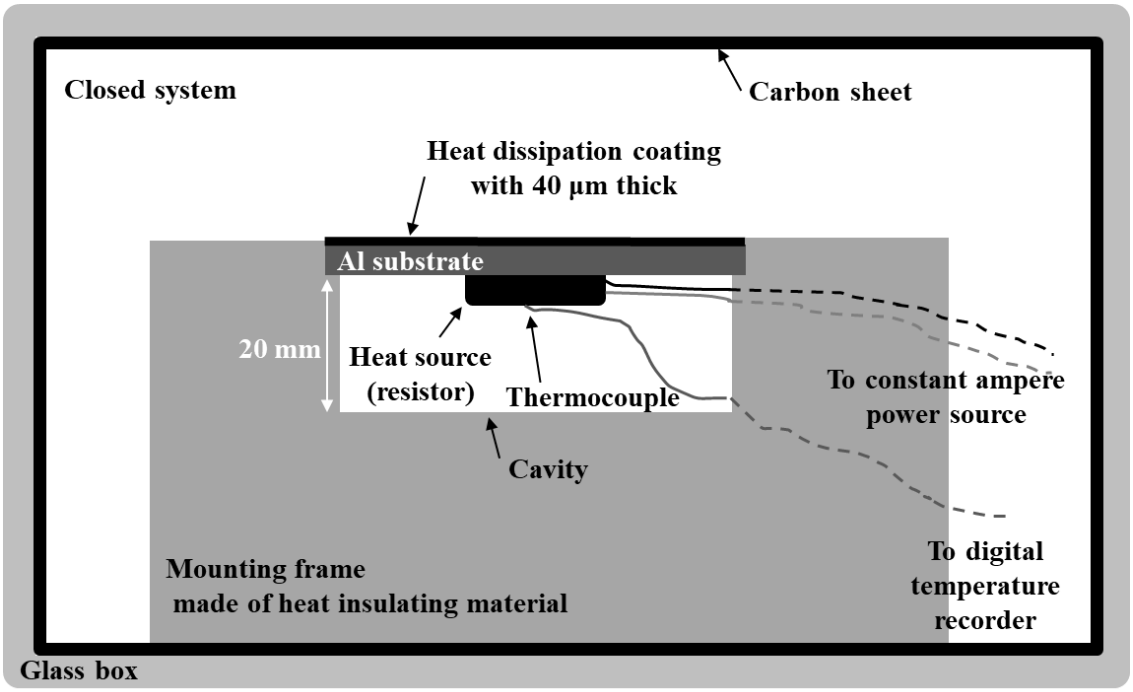

Figure 1. Schematic of the apparatus used for evaluating cooling effects of heat dissipation coatings.

A nominal constant electrical current was applied to the resistor from a constant-amperage power source. The applied current was 1.5–3.2 A. As a result, the surface temperature of the uncoated Al substrate was controlled between 310 and 400 K.

Thermocouples were attached to the surfaces of the resistor. The surface temperature was measured for 2 h after a constant electric current was applied to the resistor. The ambient temperature and humidity were 293–295 K and 45% RH, respectively. These atmospheric conditions remained nearly constant throughout the measurements. The surface temperature gradually increased and reached a steady state after 2 h, as shown in Figure 2. The temperature differences between uncoated and coated Al substrates were evaluated as heat dissipation effects.

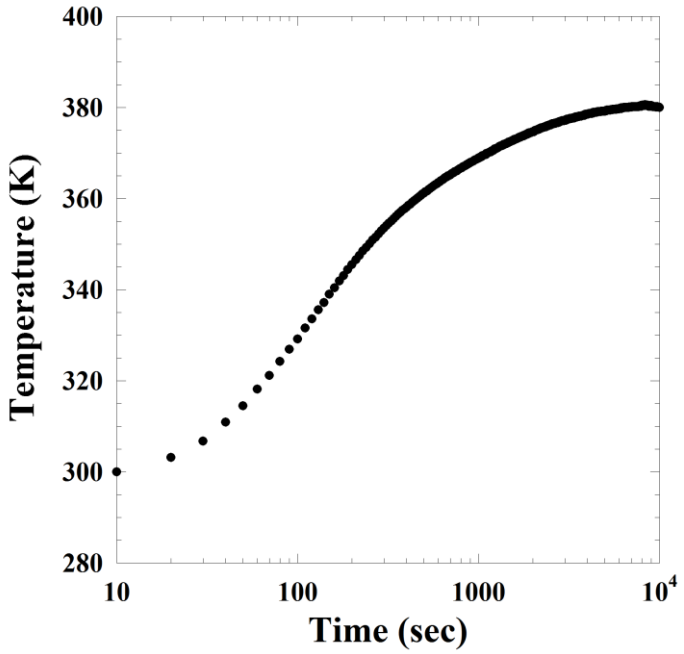

Figure 2. Time dependence of surface temperature of the resistor as a heat source after application of constant electric current (3.2 A for the coating with p-BN).

3. Results and discussion

Figure 3 shows a cross-sectional SEM micrograph of the heat dissipation coating film with CaF_2 as infrared-emitting fillers. CaF_2 particles reaching 20 μm in size were distributed within the film. The coating film was roughly packed with the fillers; the designated volume fraction of the binder resin was ~50 vol%. The surface roughness is strongly affected by the film thickness, filler particle size, and filler content. The surface area of the filler-free acrylic coating is almost equal to the nominal area of the Al substrate; with the addition of CaF_2 fillers, it is increased to between three and five times the nominal area.

Figure 4 shows the infrared emissivity as a function of wavelength for the CaF_2 particulates and the acrylic resin. Distinctive infrared emission for CaF_2 was observed in the wavelength range from 8.2 to 11.5 μm. The highest peak of ~70% occurred at 9.4 μm. Additional emission of ~40% occurred between 13.0 and 13.5 μm, whereas little emission appeared for wavelengths <8 μm. Compared to that of CaF_2, the infrared emission of the resin was much smaller. Figure 5 shows the

infrared emissivity as a function of wavelength for the p-BN and SiC particulates. These particles have characteristic emission profiles differing from that of CaF_2. p-BN exhibited sharp and strong emission for wavelengths in the range from 6.2 to 8.0 μm. An peak of ~90% appeared at 7.3 μm. Additional peaks reaching 35% are observed in the range between 12.1 and 13.2 μm. Very few materials show such selective infrared emission for wavelengths <8.0 μm. Meanwhile, for SiC, no distinctive peaks appear below 10.0 μm, but strong peaks occur for wavelengths >10.3 μm. The two peaks at ~12.0 and 13.0 μm showed ~58% and ~90% emission, respectively.

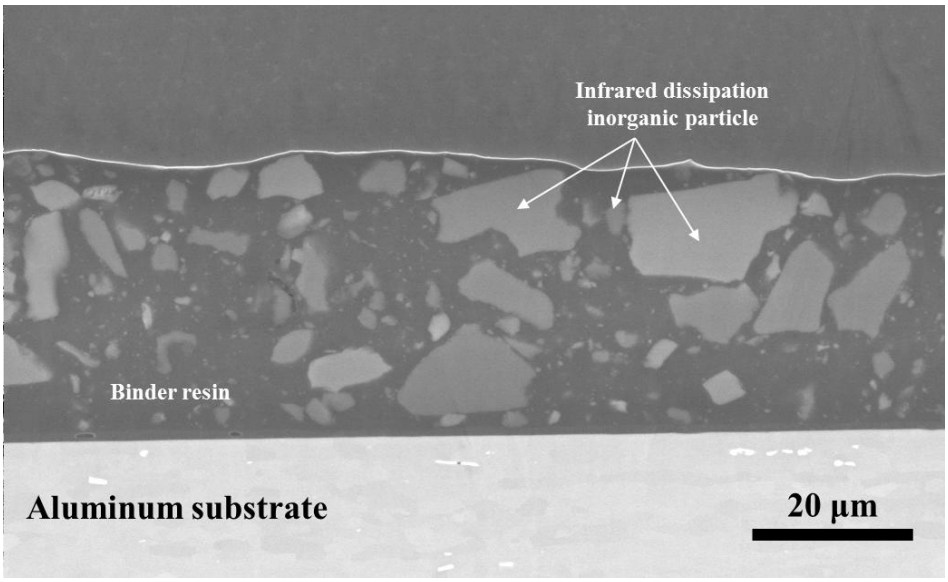

Figure 3. Typical cross-sectional SEM of microstructure of the heat dissipation coating film with CaF_2 particles on Al substrate.

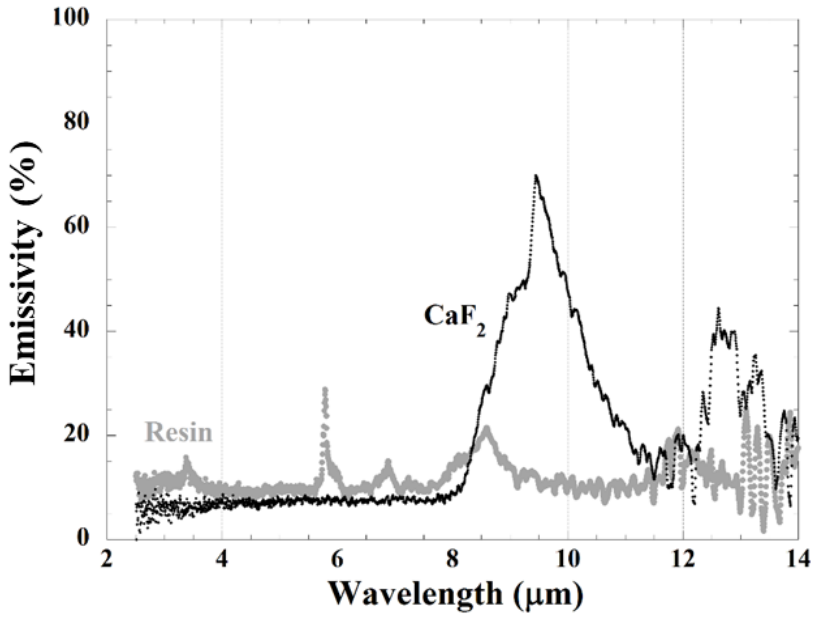

Figure 4. FT-IR spectra of CaF_2 particulates and acrylic resin.

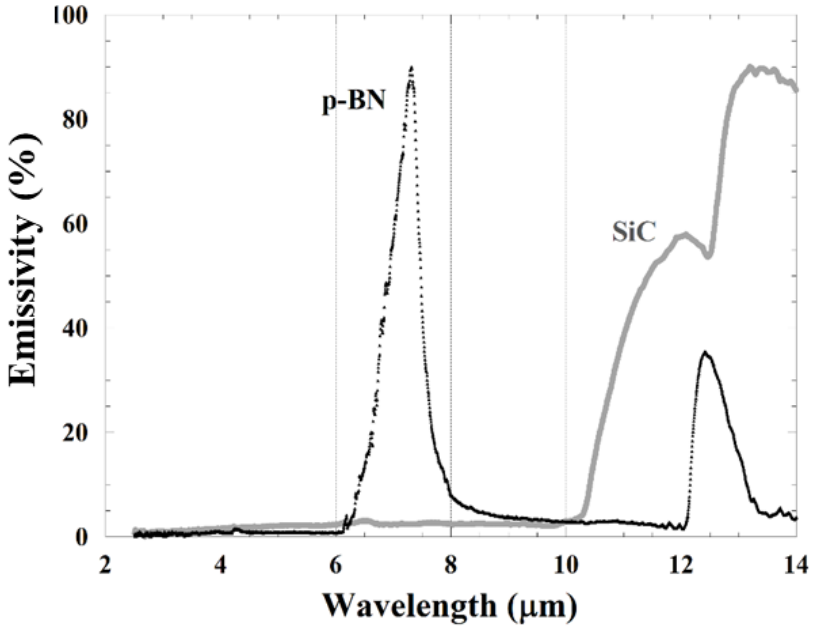

Figure 5. FT-IR spectra of p-BN and SiC particulates.

Figure 6 shows the electric current dependence of the surface temperatures at the resistor for uncoated, resin-coated, and inorganic filler-containing heat dissipation film-coated Al substrates.

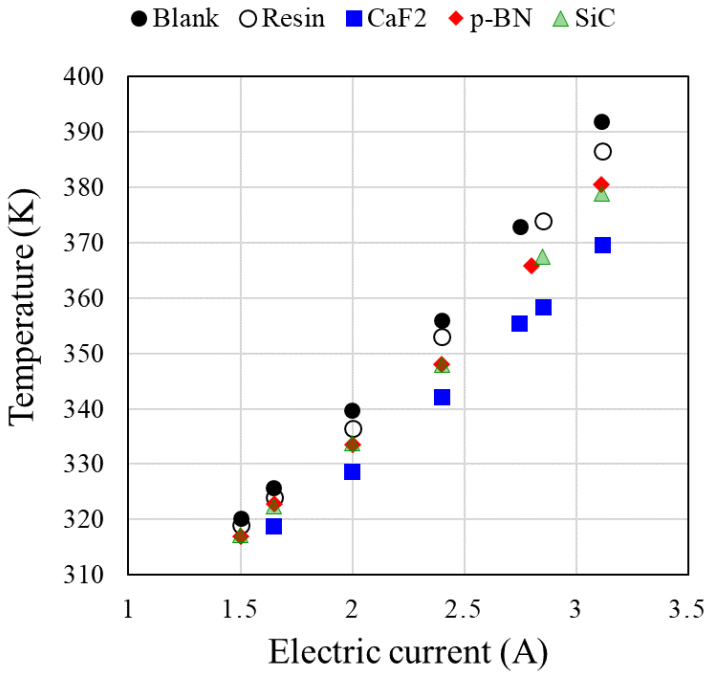

Figure 6. Change of temperature depending on the applied electric currents at the surface of the resistor for uncoated Al, acrylic resin-coated Al, and Al plates with heat dissipation coatings containing CaF_2, p-BN, and SiC particles.

With increases in the electric current, the temperatures increased almost linearly. Larger temperature reductions for heat dissipation film-coated substrates were observed in higher temperature ranges, at which higher electric currents were applied. Prominent temperature reductions were obtained for the sample with the heat dissipation coating containing CaF_2. With CaF_2 particles, the temperature was reduced to 355.5 K at 2.75 A, indicating a cooling effect of 17.4 K for conditions in which the blank Al plate reached 372.9 K. For further increases in the electric current, the temperature reduction reached 22.2 K at 3.11 A; the reduction was diminished to no more than 6.8 K at 1.65 A. Compared to that with CaF_2, the temperature reductions at the surface of the resistor were smaller for p-BN and SiC, but larger than that of the acrylic coating without any inorganic filler. Almost identical cooling effects for p-BN and SiC were obtained: approximately 8 and 3 K reduction at 2.75 and 1.65 A, respectively.

Most thermal energy generated in the resistor is transported to the Al plate and then the coating films via thermal conduction, and thereafter carried away by radiation and convection from the top surface out of the system. Convective cooling at the resistor surface is not expected in the closed and confined thermally insulated space shown in Figure 1. This is because convective heat transfer from the surface is dominated by the difference in temperature between the film surface and the ambient air and the heat transfer coefficient.

Figure 7 shows the result of a simple calculation regarding the total heat flux per unit area emitting from a coating film, Q_{total}, and the contributions of convection, $Q_{\text{convection}}$, and radiation, $Q_{\text{radiation}}$, at each temperature using the following equation:

$$Q_{\text{total}} = Q_{\text{convection}} + Q_{\text{radiation}} = a\{h(T - T_{\text{carbon}}) + f \cdot \varepsilon_{\text{f}} \cdot \sigma(T^4 - T_{\text{carbon}}^4)\} \quad (1)$$

where a, h, T, T_{carbon}, f, ε_{f}, and σ represent, respectively, the surface roughness factor, heat transfer coefficient, heat source temperature, carbon sheet temperature in the measurement system used in this study, view factor, emissivity of the heat dissipation coating, and the Stefan–Boltzmann constant of 5.67×10^{-8} W m^{-2} K^{-4}. Assuming that a = 5, h = 10 W m^{-2} K^{-1}, T_{carbon} = 294 K, and ε_{f} = 0.9, $Q_{\text{radiation}}$ becomes equivalent to $Q_{\text{convection}}$ at ~423 K [38]. Since the inflow energy from the outside of the measurement system was negligibly small compared to the heat radiation from the coating, f was approximated by 1. Although the contribution of radiation in the low-temperature region is small, radiation adds to the effects of convection and some cooling can be expected by radiative heat transfer.

The differences in temperature reduction at the resistor surface can be attributed to the differences in additional radiative effects induced by the inorganic fillers. The specific infrared emission properties of the inorganic fillers have important roles in determining the temperature-dependent cooling effects. Figure 8 shows the temperature dependence of the wavelength corresponding to the maximum radiation intensity, λ_{max}, in accordance with Wien's displacement law as follows.

$$\lambda_{\text{max}} = \frac{0.002898}{T} \quad (2)$$

As the temperature T increases, the wavelength of electromagnetic waves emitted from the object is shifted from longer to shorter values. For a given temperature, a specific wavelength exists that has the maximum intensity of radiant energy density in accordance with Planck's distribution law of radiation. Therefore, a material with the appropriate infrared emission properties must be

selected in order to dissipate thermal energy efficiently at the temperature of the object to be cooled.

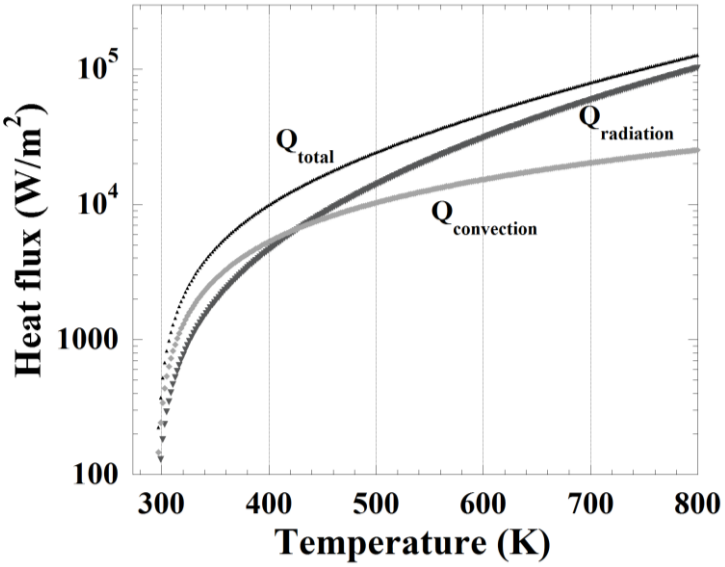

Figure 7. Temperature dependence of calculated heat flux attributed to convection, heat radiation, and their total.

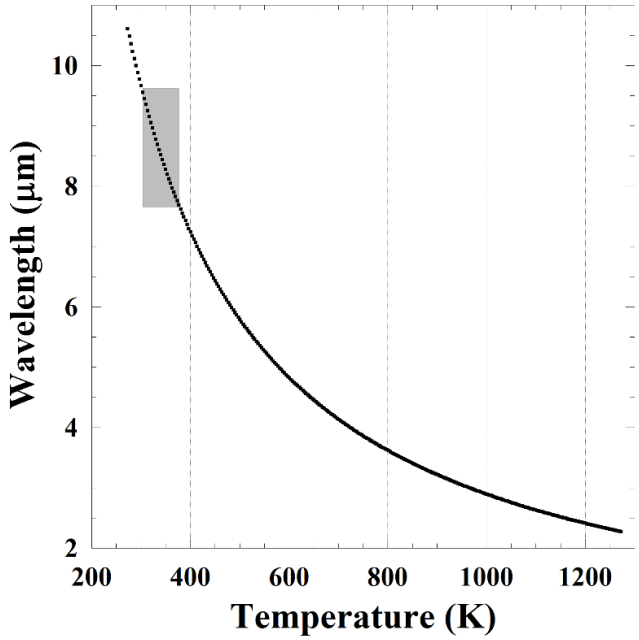

Figure 8. Temperature dependence of wavelength of maximum radiation intensity.

The inset of the gray region in Figure 8 shows the range relating to the temperature and the wavelength in consideration of this study. Materials with specific infrared radiation at ~7.8 μm for 373 K and at 9.3 μm for 313 K can provide proper radiative effects, because the emissivity and absorptivity of any solid material are equivalent. Thus, CaF_2, which exhibits distinctive broad emission in the wavelength range from 8.2 to 11.5 μm with a peak at 9.4 μm, is suitable for heat

dissipation in the relatively low-temperature region less than 373 K. Meanwhile, p-BN and SiC, which show indistinct emission in the wavelength range between 8.0 and 10.3 μm, are unfavorable for radiative heat dissipation in the same temperature range. The acrylic resin also has radiative effects, but its contribution is small, as the infrared emission of the resin is relatively insignificant in the wavelength region corresponding to the low-temperature range.

Carbon black with high total emissivity can efficiently radiate heat in the entire wavelength range. On the other hand, carbon black absorbs heat in a wide wavelength range and becomes a heat absorber that most efficiently absorbs heat radiation from the surroundings. In the absence of heat sources in the surroundings, carbon black is considered to be the most efficient heat dissipation material. However, when there are heat sources in various temperature ranges in the surroundings like the recently integrated device package, the heat dissipation coating with selective emissivity does not absorb the heat in a wide temperature ranges (absorbs the selective temperature range), but carbon black absorbs the heat with wide range. In the device design, when the temperature of the object to be cooled is limited around 80 ℃, heat can be emitted without notable inferiority as compared with carbon black even when the heat dissipation coating with selective emissivity is used because it has very high emissivity in the temperature range around 80 ℃. Under special circumstances such as device packages, the heat dissipation coating with selective emissivity may be an advantageous heat radiating material as compared with carbon black because it does not absorb extra heat. Furthermore, although the color of the heat dissipation coating with carbon black is black, it for the heat dissipation coating with selective emissivity based on CaF_2 is white. In a report so far, it has been reported that the black coating predominantly had poor heat reduction characteristics when comparing the photovoltaic modules with the carbon type black and the ceramic type white coatings [39]. This is due to efficient light absorption from the surrounding environment. It is considered that by using the heat dissipation coating with selective emissivity according to the temperature range of the heat radiation body, the thermal energy of the heat source can be released and the temperature can be effectively lowered while suppressing heat absorption from the surroundings.

To improve the lifetimes of electronic devices, reducing the operating temperature is important. As shown in Figure 6, the coatings containing inorganic particles exhibited larger temperature reductions on the resistor surfaces than those of the blank Al plate and the coating without fillers. These facts imply that the heat dissipation coatings utilizing radiative effects do provide effective cooling, and thereby extend the device lifetimes and improve reliability and performance. In particular, closed and confined systems can efficiently utilize radiative heat dissipation.

According to Kirchhoff's law, if a coating contains multiple materials with equivalent infrared emission properties, the electromagnetic wave emitted by one component is absorbed by the others. Therefore, the two-dimensional effective surface area, rather than the volume, of the heat-emitting material is important. This implies that higher filler packing contents are unnecessary; a heat dissipation coating film containing components without overlapping infrared emission properties is preferable.

In heat dissipation coatings, radiation caused by inorganic fillers, as well as convection, contributes to the cooling effect. It is necessary to select an appropriate filler material with specific infrared emission properties corresponding to the emitting wavelength at the given temperature of the objects to be cooled. It is presumed that p-BN, with distinctive short-wavelength infrared emission, and SiC, with large long-wavelength absorption, are suitable heat radiative fillers in higher

and lower temperature regimes, respectively.

Durability tests for the coating were conducted. The heat dissipation coating containing CaF_2 was coated on Al substrate. High temperature test (423 K, 3000 hours), salt spray test (240 hours according to JIS5600-7-1), light irradiation test (100 W/m^2, 333 K, 65% humidity, 5000 hours), high temperature high humidity test (358 K, 85% humidity), and heat cycle test (233 K and 393 K, 30 minutes each, 6000 cycles) were carried out. After the durability tests, the samples were heated and the temperature differences between the blank sample without coating and the samples before and after each test were compared. Table 2 shows the temperature deference (ΔT_1) for each sample. The temperature difference did not change before and after the durability test. Degradation was not observed in the radiation performance.

Table 2. Temperature differences (ΔT_1) between the blank sample without coating and the samples before and after each test.

	Before test	After high temperature test	After salt spray test	After light irradiation test	After high temperature high humidity test	After heat cycle test
ΔT_1 (K)	−12.0	−12.2	−12.0	−12.1	−11.8	−11.9

Considering the practical using, the heat dissipation characteristics when dust adhered to the coating were studied. The heat dissipation coating containing CaF_2 was coated on Al substrate. The heat dissipation characteristics of the sample adhering muddy water on the coating and drying in an oven were evaluated. The thickness of the mud was approximately 1 mm. Figure 9 shows the image after adhering mud on the sample. After attaching mud, the temperature differences between the blank sample without coating and the samples with and without mud were compared. Table 3 shows the temperature deference (ΔT_2) for each sample.

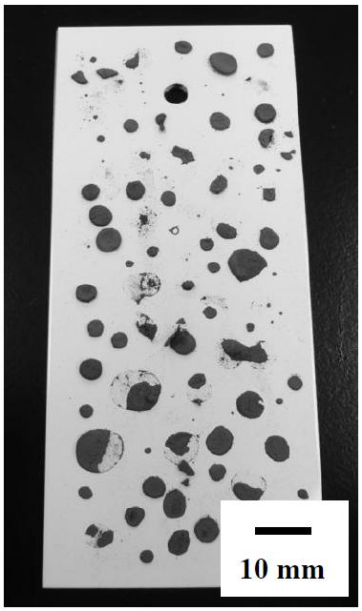

Figure 9. Image after adhering mud on the sample.

Table 3. Temperature differences (ΔT_2) between the blank sample without coating and the samples with and without mud.

	Without mud	With mud
ΔT_2 (K)	−11.8	−11.7

The temperature difference did not change for the samples with and without mud. The heat dissipation performance was similar before and after adhering mud. It is considered that because the emission wavelength of the heat dissipation coating differs from the absorption wavelength of the mud, the mud does not hinder the heat radiation from the coating.

4. Conclusions

The cooling effects of heat dissipation coating films containing infrared-absorbing inorganic fillers were studied in the temperature range from 310 to 400 K. A significant temperature reduction of about 17 K was obtained at the surface of a heat source with an acrylic coating film including CaF_2 particles on an Al plate; under equivalent conditions, the uncoated Al plate temperature reached 373 K. The cooling effect was achieved by radiative cooling, induced by the characteristic infrared absorption and emission properties of the filler materials as evaluated by FT-IR spectra. The CaF_2 particles exhibited absorption in the wavelength range from 8.2 to 11.5 μm with a strong peak at 9.4 μm, representing appropriate infrared emission properties for radiative heat dissipation at the low-temperature range. Meanwhile, coatings with p-BN and SiC, which do not feature emission in the wavelength range between 8.0 and 10.3 μm, showed inferior cooling effects to coatings with CaF_2. The results indicate that the infrared emission properties in a specific range of wavelengths pertinent to the given temperature range of the object to be cooled when considering heat dissipation coatings. This suggests that the performance of electric components could be improved by suppressing increases in temperature by using radiative heat dissipation coatings with appropriate infrared absorption and emission fillers, even at temperatures below 400 K.

Acknowledgments

The authors wish to thank Yasutaka Morozumi of Pelnox Ltd. for sample preparation and help in experiments.

Conflict of interest

The authors declare no conflict of interest related to the content of this publication.

References

1. Chang MH, Das D, Varde PV, et al. (2012) Light emitting diodes reliability review. *Microelectron Reliab* 52: 762–782.

2. Jakhar S, Soni MS, Gakkhar N (2016) Historical and recent development of concentrating photovoltaic cooling technologies. *Renew Sust Energ Rev* 60: 41–59.
3. Lall P, Pecht M, Hakim EB (1995) Characterization of functional relationship between temperature and microelectronic reliability. *Microelectron Reliab* 35: 377–402.
4. Meneghini M, Dal Lago M, Trivellin N, et al. (2012) Chip and package-related degradation of high power white LEDs. *Microelectron Reliab* 52: 804–812.
5. Zhao R, Zhang S, Liu J, et al. (2015) A review of thermal performance improving methods of lithium ion battery: Electrode modification and thermal management system. *J Power Sources* 299: 557–577.
6. Baby R, Balaji C (2012) Experimental investigations on phase change material based finned heat sinks for electronic equipment cooling. *Int J Heat Mass Tran* 55: 1642–1649.
7. Goli P, Legedza S, Dhar A, et al. (2014) Graphene-enhanced hybrid phase change materials for thermal management of Li-ion batteries. *J Power Sources* 248: 37–43.
8. Mills A, Farid M, Selman JR, et al. (2006) Thermal conductivity enhancement of phase change materials using a graphite matrix. *Appl Therm Eng* 26: 1652–1661.
9. Tan FL, Tso CP (2004) Cooling of mobile electronic devices using phase change materials. *Appl Therm Eng* 24: 159–169.
10. Micheli L, Fernández EF, Almonacid F, et al. (2016) Performance, limits and economic perspectives for passive cooling of high concentrator photovoltaics. *Sol Energ Mat Sol C* 153: 164–178.
11. Nagano H, Ohnishi A, Nagasaka Y (2001) Thermophysical properties of high-thermal-conductivity graphite sheets for spacecraft thermal design. *J Thermophys Heat Tr* 15: 347–353.
12. Nemoto E, Gunji T, Yamashita K, et al. (2009) Simultaneous separation measurement of principal thermal conductivities and principal axis angle of pyrolytic graphite sheet for two-dimensional anisotropic material using integrated multi-temperature probe method. *Jpn J Appl Phys* 48: 05EB03.
13. Wen CY, Huang GW (2008) Application of a thermally conductive pyrolytic graphite sheet to thermal management of a PEM fuel cell. *J Power Sources* 178: 132–140.
14. Zhou H, Zhu J, Liu Z, et al. (2014) High thermal conductivity of suspended few-layer hexagonal boron nitride sheets. *Nano Res* 7: 1232–1240.
15. Aliev AE, Lima MH, Silverman EM, et al. (2010) Thermal conductivity of multi-walled carbon nanotube sheets: radiation losses and quenching of phonon modes. *Nanotechnology* 21: 035709.
16. Che J, Çağın T, Deng W, et al. (2000) Thermal conductivity of diamond and related materials from molecular dynamics simulations. *J Chem Phys* 113: 6888–6900.
17. Che J, Çagin T, Goddard III WA (2000) Thermal conductivity of carbon nanotubes. *Nanotechnology* 11: 65.
18. Inagaki M, Kaburagi Y, Hishiyama Y (2014) Thermal management material: graphite. *Adv Eng Mater* 16: 494–506.
19. Kidalov S, Shakhov F (2009) Thermal conductivity of diamond composites. *Materials* 2: 2467–2495.
20. Varshney V, Patnaik SS, Roy AK, et al. (2010) Modeling of thermal transport in pillared-graphene architectures. *ACS Nano* 4: 1153–1161.

21. Zhang G, Jiang S, Yao W, et al. (2016) Enhancement of natural convection by carbon nanotube films covered microchannel-surface for passive electronic cooling devices. *ACS Appl Mater Inter* 8: 31202–31211.
22. Walsh E, Grimes R (2007) Low profile fan and heat sink thermal management solution for portable applications. *Int J Therm Sci* 46: 1182–1190.
23. Bao H, Yan C, Wang B, et al. (2017) Double-layer nanoparticle-based coatings for efficient terrestrial radiative cooling. *Sol Energ Mat Sol C* 168: 78–84.
24. Chen Z, Zhu L, Raman A, et al. (2016) Radiative cooling to deep sub-freezing temperatures through a 24-h day–night cycle. *Nature Commun* 7: 13729.
25. Granqvist CG, Hjortsberg A (1981) Radiative cooling to low temperatures: General considerations and application to selectively emitting SiO films. *J Appl Phys* 52: 4205–4220.
26. Hossain MM, Gu M (2016) Radiative cooling: principles, progress, and potentials. *Adv Sci* 3: 1500360.
27. Kecebas MA, Menguc MP, Kosar A, et al. (2017) Passive radiative cooling design with broadband optical thin-film filters. *J Quant Spectrosc Ra* 198: 179–186.
28. Huang Z, Ruan X (2017) Nanoparticle embedded double-layer coating for daytime radiative cooling. *Int J Heat Mass Tran* 104: 890–896.
29. Kou JL, Jurado Z, Chen Z, et al. (2017) Daytime radiative cooling using near-black infrared emitters. *ACS Photonics* 4: 626–630.
30. Raman AP, Anoma MA, Zhu L, et al. (2014) Passive radiative cooling below ambient air temperature under direct sunlight. *Nature* 515: 540–544.
31. Nishioka K, Ota Y, Tamura K, et al. (2013) Heat reduction of concentrator photovoltaic module using high radiation coating. *Surf Coat Tech* 215: 472–475.
32. Chen H, Ginzburg VV, Yang J, et al. (2016) Thermal conductivity of polymer-based composites: Fundamentals and applications. *Prog Polym Sci* 59: 41–85.
33. Choi S, Kim J (2013) Thermal conductivity of epoxy composites with a binary-particle system of aluminum oxide and aluminum nitride fillers. *Compos Part B-Eng* 51: 140–147.
34. Hashim NH, Anithambigai P, Mutharasu D (2015) Thermal characterization of high power LED with ceramic particles filled thermal paste for effective heat dissipation. *Microelectron Reliab* 55: 383–388.
35. Shao Y, Shi FG (2017) Passive cooling enabled by polymer composite coating: Dependence on filler, filler size and coating thickness. *J Electron Mater* 46: 4057–4061.
36. Tsuda S, Shimizu M, Iguchi F, et al. (2017) Enhanced thermal transport in polymers with an infrared-selective thermal emitter for electronics cooling. *Appl Therm Eng* 113: 112–119.
37. Yuan C, Li L, Duan B, et al. (2016) Locally reinforced polymer-based composites for efficient heat dissipation of local heat source. *Int J Therm Sci* 102: 202–209.
38. Bird RB, Stewart WE, Lightfoot EN (1960) *Transport Phenomena*, John Wiley & Sons, Inc.
39. Nishioka K, Araki K, Ota Y, et al. (2011) Heat release effect of high radiation layer coated on aluminum chassis of concentrator photovoltaic module. *7th International Conference on concentrating Photovoltaic Systems*.

AIMS Press